ELSEVIER

Journal of Molecular Structure (Theochem) 493 (1999) 275–285

THEO CHEM

www.elsevier.nl/locate/theochem

Isomers of adenine

J. Vega, K. Michaelian[a,b,*], I.L. Garzón[b], M.R. Beltrán[c], L. Hernández[d]

[a]*Facultad de Ciencias, UNAM, 04000 México, D.F., Mexico*
[b]*Instituto de Física, UNAM, A.P. 20-364, 01000 México, D.F., Mexico*
[c]*Instituto de Investigaciones en Materiales, UNAM, A.P. 70-360 México, D.F., Mexico*
[d]*Instituto Superior de Ciencias y Tecnologias Nucleares, A.P. 6163, Habana 10600, Cuba*

Received 23 September 1998; received in revised form 23 March 1999; accepted 2 July 1999

Abstract

Adenine is one of the four principle bases of nucleic acid, the essential molecule of life and evolution. Apparently, only one configuration of adenine exists in nature giving it unique chemical and biological properties. Using a force field type potential model with parameters fitted to the nucleic acid bases, proteins and other biological molecules (involving the sum of the contributions from bond stretching, bond angle bending, torsional angle twisting, and Coulomb and Lennard–Jones terms) we searched the potential energy surface for other stable isomers of adenine. The search was performed using a genetic algorithm, an efficient and global technique. The most interesting of the lowest energy minima found in the global search were relaxed using quantum-mechanical, semiempirical (PM3), and first principles (Hartree–Fock and density functional theory) methods. These calculations gave similar geometries and energy ordering for the new structures. This work formed part of a larger project to study the binding of nanoclusters of gold to segments of nucleic acid for possible application in the emerging field of nano-electronics. The results could also have implications in mutation and transcription of DNA.

Keywords: Adenine; DNA; Genetic algorithms; Ab initio; Nano-electronics

1. Introduction

The microscopic structure of DNA with its phosphate, sugar and base pair components is recently receiving a lot of attention since computing power and first principles calculations have matured to such an extent that ab initio calculations with segments of DNA containing a very large number of atoms are now feasible [1]. Understanding how the tertiary structure of DNA affects its chemical and biological characteristics is a goal of biochemists now within sight. Also, new DNA handling and genetic engineering capabilities have given rise to a host of intriguing possibilities ranging from disease correction to nano-electronic circuits with transistors made of metal nanoclusters connected through segments of DNA [2–5].

Single bases of DNA and their pairing through hydrogen bonds in their “natural” conformations has been studied in significant detail through first principles calculations such as ab initio SCF [6] and density functional theory [7]. Comparison with the experimental values is, generally, very good. The logical

* Corresponding author.
E-mail addresses: karo@fenix.ifisicacu.unam.mx (K. Michaelian), vega@fenix.ifisicacu.unam.mx (J. Vega), lisandro@isctn.edu.cu (L. Hernandez)

0166-1280/99/$ - see front matter
PII: S0166-1280(99)00249-3

next step in this line of investigation is the simulation of sets of base pairs connected to the phosphate and sugar backbone, i.e. segments of DNA.

The work presented in this article, however, has a different focus. We were not interested in the "natural" configuration but in the possible isomers of the bases. Are there in fact other stable isomers of the bases and if so, why is there apparently only one configuration found for each base in nature? Or, is this just due to lack of experimental data? If there are isomers, how probable are they in nature, and could these isomers have importance in mutation and transcription? The existence of different isomers of the bases would also have significance in the field of nano-electronics where the electrical properties of a component would be sensitive to the metal cluster–DNA interface.

Previous works on the bases and their pairs have thus been concerned with the structural and electronic properties of only their "natural" configuration. Experimentally obtained coordinates of the atoms of the bases were input to ab initio codes and only local optimization was performed. In this work we perform a truly global search using the potential model with the object of finding stable minima which are distinct from the "natural" configuration. As a starting point, we study one of the four principle bases of DNA, adenine.

Because of the extensive CPU time required to globally optimize with ab initio calculations, we take the approach of using a potential model to obtain a quick but "complete" survey of the potential energy surface using a global genetic search algorithm. The interesting minima found with this technique are further studied with a semiempirical approach, PM3, and two different types of first principle calculations, Hartree–Fock and density functional theory.

In the following section we describe the potential model and in Section 3 the global search algorithm is described. In Section 4 we describe the PM3, Hartree–Fock and density functional local optimizations of the interesting configurations found with the global potential approach. In Section 5 we give the results and Section 6 presents the conclusions, implications and future directions of this work.

2. The force field potential

Over the last 15 years, a large effort has been put into obtaining analytical forms for potential energy functions, which can correctly describe the structure, energetics and vibrational frequencies of complex biological macromolecular systems. Most of the effort has been applied to proteins; more recently, potential functions have been developed for nucleic acids and have even been employed in dynamical simulations. The potential energy function we used was developed by Weiner et al. [8] for the simulation of nucleic acids and proteins. This function is an extension of a force field which used a united atom (spherical) representation of the CH, CH_2 and CH_3 groups [9]. The potential energy function allows a general all atom representation of nucleic acids and proteins and has the following form

$$V = \sum_{\text{bonds}} K_R(R - R_0)^2 + \sum_{\text{angles}} K_\theta(\theta - \theta_0)^2 + \sum_{\text{dihedral angles}} \frac{V_n}{2}[1 + \cos(n\phi - \gamma)] + \sum_{i<j}\left[\frac{A_{ij}}{R_{ij}^{12}} - \frac{B_{ij}}{R_{ij}^{6}} + \frac{332.17 q_i q_j}{\varepsilon R_{ij}}\right] + \sum_{\text{H-bonds}}\left[\frac{C_{ij}}{R_{ij}^{12}} - \frac{D_{ij}}{R_{ij}^{10}}\right] \quad (1)$$

where R, K_R and R_0 are the bond length, bond stretch force constant, and equilibrium distance, respectively, for the covalently bonded atoms; $\theta, K_\theta, \theta_0$ are the bond angle, angle bend force constant and equilibrium angle, respectively, for the angles between the covalent bonds of a given atom. A Fourier expansion of the torsional energy in terms of the dihedral angle ϕ is implied. $V_n/2$ is the force constant, n is the multiplicity of the expansion and γ is a phase value. Together, the first three terms account for variations in the covalent bonding energy of the molecule.

The fourth term is the non-bonded term and represents the van der Waals (Lennard–Jones) and electrostatic energies. The quantities R_{ij}, q_i and q_j are the non-bonded distances and the charges, respectively, for the atom pair i and j. The atom centered charges q_i were derived by Weiner et al. [8] by using quantum

mechanically derived electrostatic potentials fit to a point charge model. Charge neutrality was then enforced by distributing the excess charge to the same ratios as that found from Mulliken populations [9]. The factor ε is an effective dielectric parameter, $\varepsilon = r_{ij}$, which mimics polarization effects in attractive interactions [10]. The last term is the hydrogen-bond energy, which provides the union of the relevant base pair (e.g. Adenine–Thymine and Cytosine–Guanine). Because we were not interested in the A–T pairing, we did not include hydrogen bonding. The units of V are in kcal/mol with R in angstroms, θ and ϕ in radians, q_i in electrostatic units, and 332.17 is a conversion factor.

For a description of the derivation of the values of the potential parameters from experimental data, see Refs. [8,9].

3. The global search

Finding the low energy stable structures of molecules is a difficult global optimization problem. Not withstanding the recent gains in efficiency with the maturing of ab initio molecular dynamics, global optimizations with this method are computationally taxing because of the large number of electronic degrees of freedom. Approaches employing classical potentials with parameters adjusted to either experimental data or selected ab initio results are an effective alternative. Such potentials often include effects beyond the scope of the formalism [10] and, in any case, results obtained through the classical optimization can be used as configurational input to a full ab initio or a density functional calculation.

In this work we employ a genetic algorithm with the force field potential described in Section 2 as the global search algorithm. The genetic algorithm, originally proposed by Holland [11], is based on nature's efficient problem solving method of evolving a microscopic genetic code through mutation and crossover, with selection based on the fitness of the corresponding individuals. It is an intelligent and information efficient approach [12] to multi-variable, global optimization and has been successfully applied to a large number of complex problems from the physical sciences [13]. McGrrah and Judson [14] first applied the genetic algorithm to the molecular conformation determination of the molecule cyclic hexaglycine. Judson et al. [15] have looked at the effectiveness of the GA in finding the ground state of a 2-D polymer compared to the random and simulated annealing global search approaches. They arrived at the general conclusion that the larger the molecule, the greater the effectiveness of the GA approach over the others. For large systems, we have demonstrated that a "symbiotic" variant of the genetic algorithm is still more effective than the genetic algorithm [16]. A general introduction to

Table 1
The energy and the number of times encountered of the lowest 34 stationary points found in 13 000 global optimizations of random initial configurations of the atoms of adenine using the force field potential with the genetic search algorithm

Energy (kcal/mol)	Times encountered
− 550.870860	9365
− 491.505479	9
− 488.269038	76
− 487.294911	8
− 485.160921	19
− 484.583130	18
− 481.849328	7
− 473.464861	1
− 465.108048	1
− 461.526329	103
− 459.704370	94
− 456.300295	71
− 454.158045	73
− 441.794629	152
− 435.671347	705
− 433.984435	722
− 426.316431	1
− 424.762576	1
− 418.752674	7
− 417.338110	1
− 416.453197	3
− 415.427917	1
− 414.639058	1
− 410.058122	1
− 408.055944	1
− 407.597946	2
− 405.867522	2
− 402.139537	1
− 398.501011	1
− 394.758042	1
− 392.648878	1
− 389.522938	16
− 388.604132	30
− 384.637602	12

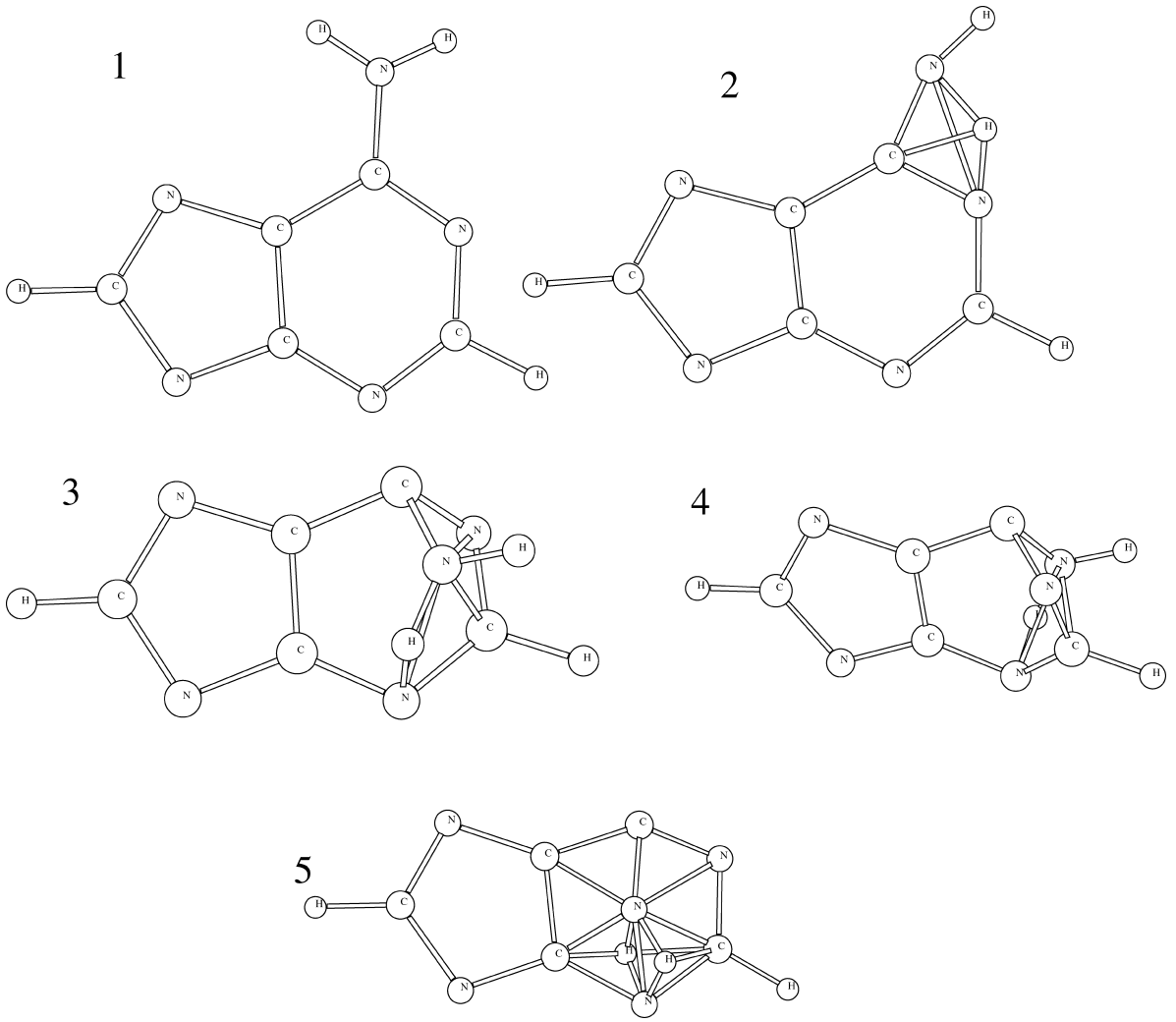

Fig. 1. The geometries of the most interesting (see text) lowest energy stable configurations found for the atoms of adenine in 13 000 global optimizations starting from random configurations. These results were obtained with the force-field potential described in Section 2.

genetic algorithms can be found in Ref. [17]. For details on the specific application of the genetic algorithm to atomic systems, see Refs. [18,19].

We begin the genetic global search by generating a population of distinct random configurations of the 14 atoms of adenine (5 of nitrogen, 5 of carbon, and 4 of hydrogen). These are generated at random positions within a sphere of radius $r = 5$ Å centered at the origin of a 3D coordinate system. This relation gives a radius somewhat larger than that of a sphere enclosing the "natural" adenine structure. A genetic string is composed for each configuration in the population [19] by locating the three spatial coordinates of each atom together, and the sets of coordinates of each atom are ordered along the string in the order in which they are generated. An 8-bit binary Gray coding [20] of the coordinate variables was chosen.

The variables, corresponding to atom coordinates, are evolved with the standard genetic algorithm technique [19] employing mutation and crossover, with selection based on a fitness function for the molecule, which was the total interaction energy of the system as defined by Eq. (1). Evolution proceeds until the lowest energy for the molecule has not changed during seven

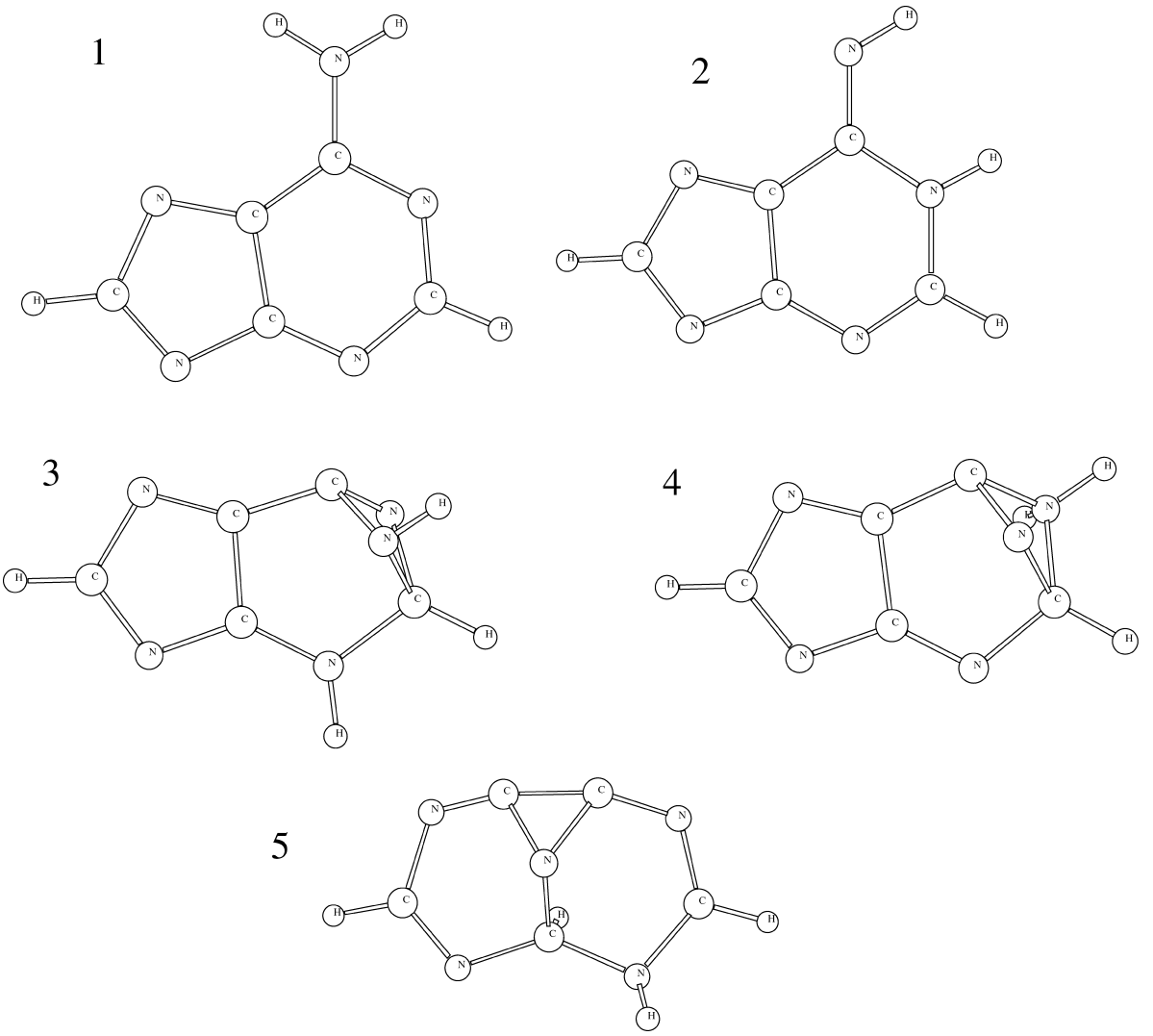

Fig. 2. The geometries of Fig. 1 after local optimization using the semiempirical PM3 calculations.

consecutive generations. At this point the configuration is in an attraction basin of a low energy local minimum and a local conjugate gradient optimization of the type Polak–Ribiere [21] is performed to refine the structural details of the molecule. The energy of the configuration was thus locally minimized in an iterative procedure to a precision of $\Delta V/V = 10^{-8}$. The stabilities of the configurations so obtained were then checked by obtaining and diagonalizing the Hessian to high numerical precision and discarding those configurations which presented negative eigenvalues.

4. Quantum mechanical calculations

Three distinct quantum calculations, PM3, Hartree–Fock, and density functional theory were employed in a local optimization of the interesting configurations found with the potential model. The MNDO-PM3 method uses a semiempirical, self-consistent field-molecular orbitals (SCF-MO) Hamiltonian [22] parametrized using the standard heats of formation of a large set of reference molecules [23]. It is designed to reproduce the standard

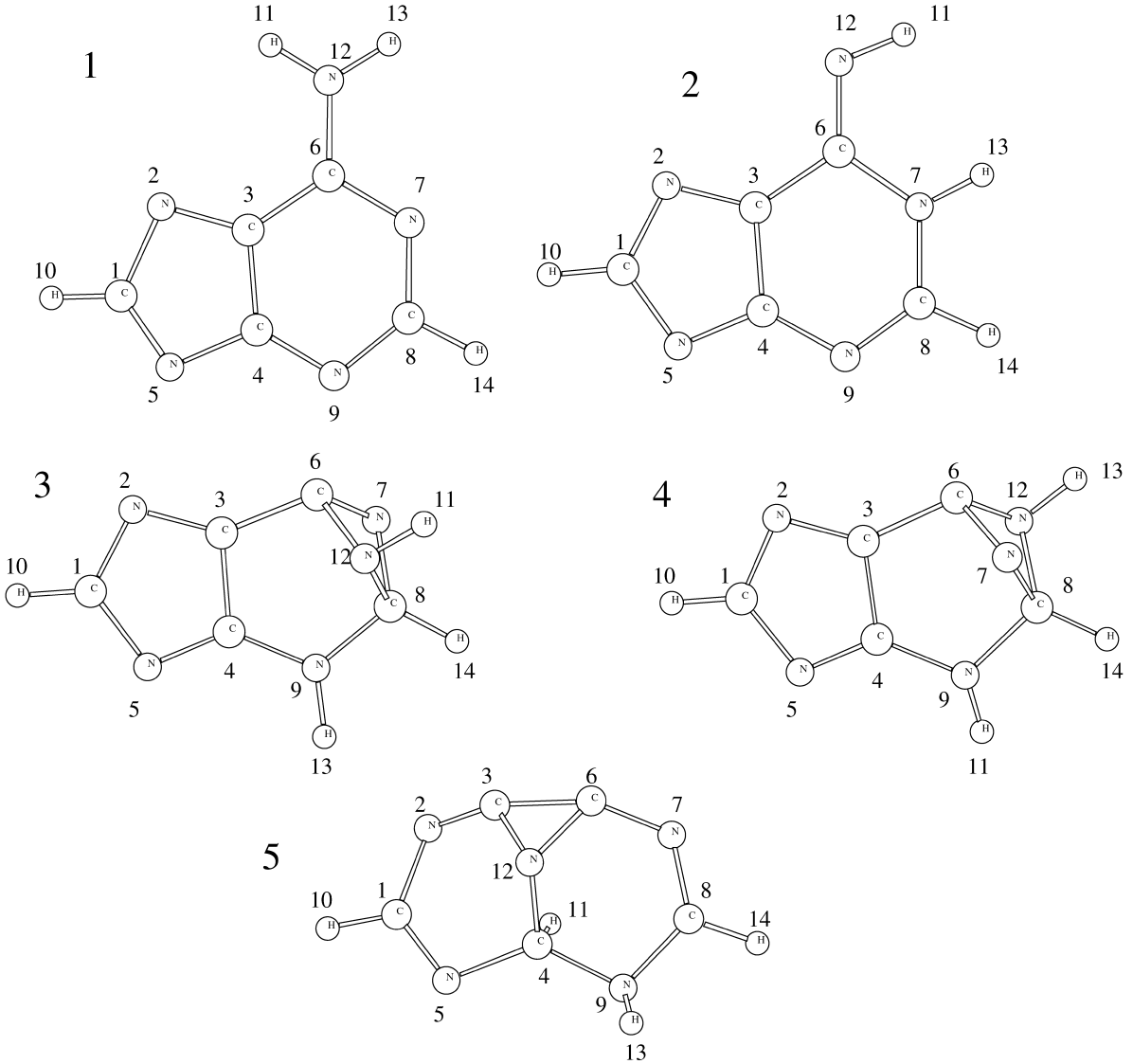

Fig. 3. The geometries of Fig. 1 after local optimization using the Hartree–Fock calculations.

heats of formation from total energies (with inclusion of accurate experimental atomization heats) for molecular geometries corresponding to the minimal SCF value. We used a minimum basis set of Slater type orbitals (STO) to describe the valence electrons in the frozen core approximation. The method gives reliable results for the molecular orbitals and electronic affinities. The errors that arise due to the simplifications related with the MNDO approximations are partially compensated for by fitting to precise experimental data from a large set of reference molecules in their ground states. The MO and energy gradient calculations were performed with the MOPAC program [24]. Eigenvector following was the method chosen to search for the minima [25,26].

In the second set of quantum calculations, ab initio molecular orbital optimizations were carried out with the all-electron self-consistent-field Hartree–Fock-linear combination of atomic orbitals (HF-LCAO) computational scheme, as implemented in the

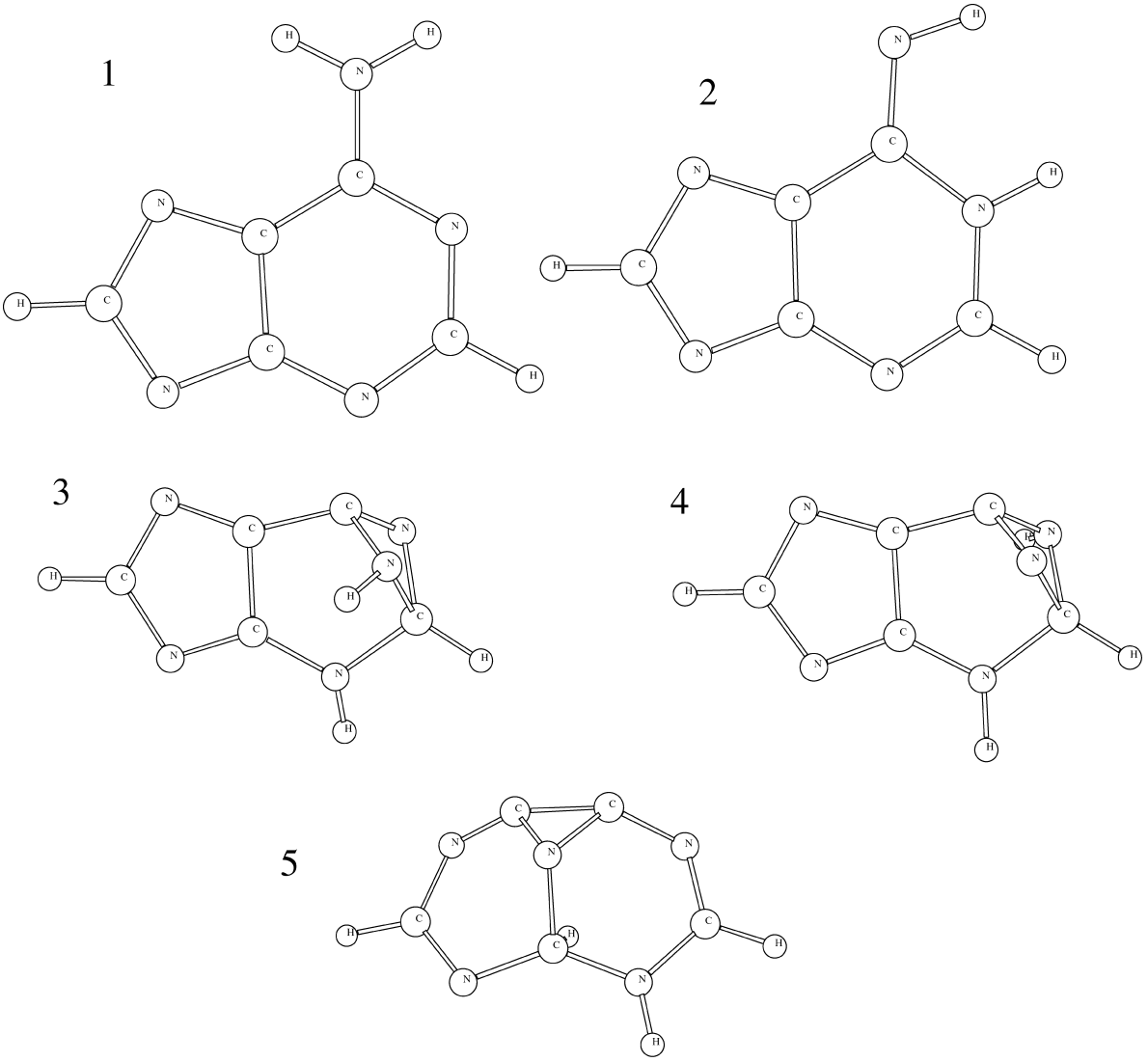

Fig. 4. The geometries of Fig. 1 after local optimization using the density functional calculations.

GAUSSIAN 94 program [27]. The diagonalization of the Hamiltonian was performed using a 6-31G* basis set. For optimization of the nuclear coordinates a Berny algorithm [28] was incorporated without imposing any symmetry constraints on the geometry. A convergence criterion in which forces were required to be less than 10^{-4} a.u. was used to stop the geometry optimization.

The third set of quantum calculations consisted of a fully self-consistent density functional theory (DFT) calculation performed to solve the standard Kohn–Sham self-consistent equations in the local density approximation (LDA) [29]. These calculations were performed using the SIESTA code [30,31]. The core electrons have been eliminated and replaced by the standard norm conserving Troullier–Martins pseudopotentials in their fully non-local (Kleinman–Bylander) form [32,33]. Flexible linear combinations of numerical (pseudo) atomic orbitals (PAO) are used as the basis set, allowing for double ζ polarization orbitals. In order to limit the range of the pseudoatomic basis orbitals, they are

Table 2
Comparison of the geometries of the "natural" configuration as locally optimized using the potential model, PM3, Hartree–Fock and density functional calculations with the experimental data from Ref. [33]. The χ^2 values of the calculations with respect to the experimental data set are given. The bond lengths are in units Å of and the angles are in degrees. See isomer 1 of Fig. 3 for the labeling of the bonds and angles

	Pot. mod.	PM3	HF	DF	Exp
Bond					
1–2	1.311	1.433	1.419	1.389	1.312
2 –3	1.409	1.356	1.332	1.338	1.385
3–4	1.379	1.468	1.414	1.457	1.382
4–5	1.391	1.433	1.414	1.375	1.376
5–1	1.393	1.327	1.269	1.343	1.367
1–10	1.143	1.096	1.071	1.098	
3–6	1.409	1.423	1.412	1.417	1.409
6–7	1.263	1.395	1.327	1.354	1.349
7–8	1.274	1.337	1.327	1.342	1.338
8–9	1.276	1.389	1.337	1.350	1.332
9–4	1.299	1.327	1.299	1.329	1.342
8–14	1.132	1.099	1.074	1.103	
6–12	1.276	1.360	1.340	1.339	1.337
12–11	0.907	0.986	0.993	1.029	
12–13	0.903	0.989	0.994	1.027	
χ^2	0.016	0.025	0.021	0.011	0.000
Angle					
1–2–3	104.47	105.13	101.89	102.33	103.9
2–3–4	110.01	108.82	109.94	109.79	110.7
3–4–5	106.81	106.38	107.56	107.64	105.7
4–5–1	105.04	105.93	103.37	103.19	105.9
5–1–2	113.66	113.74	117.24	116.85	113.8
5–1–10	123.67	125.14	123.85	122.09	
2–1–10	122.66	121.12	118.91	121.06	
9–4–5	128.60	129.59	127.72	131.71	
9–4–3	124.59	124.03	124.72	120.24	126.9
4–3–6	116.91	116.12	117.05	117.21	116.9
3–6–7	115.11	118.39	117.80	120.27	117.6
6–7–8	122.47	120.74	118.90	117.92	118.8
9–8–14	115.37	117.63	115.91	116.73	
7–8–9	129.27	124.78	128.47	126.18	129.0
8–9–4	111.65	115.95	113.06	117.85	110.8
14–8–7	115.36	117.60	115.62	117.06	
7–6–12	121.82	116.04	119.41	119.18	119.0
6–12–13	118.55	120.54	119.15	119.36	
6–12–11	120.21	119.31	120.91	118.39	
13–12–11	121.24	118.31	119.82	122.21	
χ^2	0.241	0.535	0.328	1.146	0.000

slightly excited by a common 'energy shift' ($\delta E_{\mathrm{PAO}} = 0.02$), and truncated at the resulting radial node [34]. The basis functions and the electron density are projected onto a uniform real-space grid in order to calculate the Hartree and exchange-correlation potentials and matrix elements. The grid fineness is controlled by the 'energy cutoff' ($E_{\mathrm{cut}} = 120$ Ry) of the planewaves that can be represented in it without aliasing [31]. Structural relaxation was performed using an unconstrained conjugate gradient method with the DFT-LDA forces described above to a convergence criteria of 10^{-4} a.u.

Table 3
The geometrical parameters of the isomer labeled 2 in Fig. 3 relaxed with the Hartree–Fock calculations

Bond	Å	Angle	Degrees	Torsion	Degrees
1–2	1.346	1–2–3	102.64	2–1–5–4	0.00
2–3	1.315	2–3–4	108.64	7–6–3–4	0.00
3–4	1.474	3–4–5	108.46	6–3–4–9	0.00
4–5	1.305	4–5–1	102.98	2–3–4–5	0.00
5–1	1.356	5–1–2	117.28	6–7–8–9	0.00
1–10	1.071	3–6–7	111.27	13–7–6–12	0.02
4–9	1.355	6–7–8	124.55	11–12–6–7	0.00
9–8	1.282	7–8–9	126.51	14–8–7–13	359.95
8–7	1.364	8–9–4	114.92	3–6–7–8	0.00
7–6	1.402	9–4–3	123.24		
6–3	1.433	4–3–6	119.51		
11–12	1.007	5–1–10	121.38		
14–8	1.074	13–7–6	118.10		
6–12	1.288	7–6–12	124.89		
13–7	0.996	6–12–11	112.41		
		14–8–7	114.51		

Table 4
The geometrical parameters of the isomer labeled 3 in Fig. 3 relaxed with the Hartree–Fock calculations

Bond	Å	Angle	Degrees	Torsion	Degrees
1–2	1.355	1–2–3	102.56	1–2–3–4	359.51
2–3	1.304	2–3–4	108.93	2–3–4–5	0.20
3–4	1.465	3–4–5	109.52	4–9–8–7	305.11
4–5	1.295	4–5–1	102.21	6–7–8–12	335.97
5–1	1.370	5–1–2	116.77	13–9–8–14	23.82
1–10	1.070	3–6–7	110.13	11–12–8–7	274.78
4–9	1.360	6–7–8	83.34	3–6–7–8	274.13
9–8	1.454	7–8–9	106.38	13–9–8–7	153.14
8–7	1.479	8–9–4	114.17	4–3–6–7	50.77
7–6	1.421	9–4–3	116.97		
6–3	1.484	4–3–6	109.56		
11–12	1.004	5–1–10	121.53		
12–8	1.478	11–12–8	110.54		
13–9	0.996	12–8–7	91.09		
8–14	1.079	13–9–8	119.60		
6–12	1.473	9–8–14	110.70		
		3–6–12	107.39		

5. Results

In 13 000 runs of the genetic algorithm with the potential model, starting from completely random configurations, we found more than 100 stationary points. The energy and the number of times encountered of the 34 lowest energy points is listed in Table 1. The number of times these local minima or saddle points were found is directly related to the size of their attraction basins. The lowest energy configuration found indeed corresponded to the well know "natural" configuration and this configuration was found the largest number of times, implying the largest attraction basin for the natural state.

It should be emphasized that the force field potential was fitted to experimental data from "natural" configurations. Although the number and types of molecules fitted was large, it is probable that the potential provides a good description of nature only for the natural configurations. Configurations that differ substantially from this are probably not well represented by the potential. Those configurations which therefore proved the most interesting because of their approximate geometrical correspondence to the natural state are displayed in Fig. 1. The stability of these isomers was verified by determining and diagonalizing numerically the Hessian to high numerical precision. All configurations had purely positive eigenvalues, with six eigenvalues equal to zero for the 6 degrees of translational and rotational freedom not removed during the optimization process. Most of the configurations found had a twin formed by exchanging the hydrogen atoms in the H–N–H bond. This was an artifact due to the distinct charges assigned to the two hydrogen atoms and the fact that the charges were not optimized in the potential model approach.

The atomic coordinates of the configurations of Fig. 1 were used as input to the PM3, Hartree–Fock and density functional local minimizations. The resulting relaxed configurations are given in Figs. 2–4, respectively. All configurations converged to within the required tolerance set for the respective calculations (see Section 4). The relaxed configurations are similar for the PM3 and Hartree–Fock and density functional calculations. There is, however, a slight difference in the angle of an N–H bond for isomers 3 and 4 of the density functional calculations, as is evident in comparing Figs. 3 and 4.

Table 5
The geometrical parameters of the isomer labeled 4 in Fig. 3 relaxed with the Hartree–Fock calculations

Bonds	Å	Angle	Degrees	Torsion	Degrees
1–2	1.355	1–2–3	102.57	1–2–3–4	0.54
2–3	1.304	2–3–4	108.92	3–4–5–1	359.87
3–4	1.464	3–4–5	109.54	4–9–8–12	317.53
4–5	1.295	4–5–1	102.20	3–6–12–8	271.87
5–1	1.370	5–1–2	116.77	4–3–6–7	309.25
1–10	1.070	3–6–12	107.41	9–4–3–6	5.08
4–9	1.360	6–12–8	81.66	4–3–6–12	49.98
9–8	1.453	12–8–9	109.59		
8–7	1.480	8–9–4	114.27		
7–6	1.421	9–4–3	116.91		
6–3	1.483	4–3–6	109.59		
13–12	1.004	5–1–10	121.53		
12–8	1.477	13–12–8	110.60		
11–9	0.996	12–8–7	91.09		
8–14	1.079	11–9–8	119.78		
6–12	1.473	9–8–14	110.67		
		3–6–7	110.17		

Table 2 gives a quantitative comparison of the relaxed geometries of the "natural" configuration of adenine found with the four distinct calculations and with the experimental results of [35]. The χ^2 comparisons of the calculations to the experimental data are also given in the table. Tables 3–6 list the geometrical parameters, for the Hartree–Fock calculation, of the

Table 6
The geometrical parameters of the isomer labeled 5 in Fig. 3 relaxed with the Hartree–Fock calculations

Bonds	Å	Angle	Degrees	Torsion	Degrees
1–2	1.423	1–2–3	109.47	5–4–12–6	218.09
2–3	1.286	2–1–5	124.19	4–9–8–7	8.16
5–4	1.443	5–4–12	104.70	13–9–8–14	63.12
4–12	1.455	4–12–6	102.93	8–7–6–12	356.09
12–6	1.411	4–9–8	104.91	9–4–12–6	75.11
4–9	1.431	9–8–7	125.82	12–3–2–1	1.91
9–8	1.423	13–9–8	115.01	8–9–4–12	302.27
8–7	1.304	9–8–14	115.68	1–5–4–11	300.51
13–9	1.002	8–7–6	114.75		
8–14	1.074	7–6–12	118.57		
7–6	1.374	9–4–12	107.22		
11–4	1.086	6–12–3	62.59		
12–3	1.393	1–5–4	107.13		
1–5	1.303	12–4–11	109.48		
14–8	1.074	13–9–8	115.01		
6–3	1.457	9–4–12	107.22		

Table 7
Comparison of the differences in the total energy between the natural configuration of adenine (isomer1) and the isomers of higher energy listed in Figs. 1–4 for the potential model, PM3, Hartree–Fock and density functional calculations

Isomer	Energy (kcal/mol)	Energy difference (kcal/mol)			
	Pot. mod.	Pot. mod.	PM3	HF	DF
1	− 550.871	0.0	0.0	0.0	0.0
2	− 485.161	+ 65.71	+ 12.94	+ 6.76	+ 17.75
3	− 435.671	+ 115.20	+ 93.73	+ 98.13	+ 96.41
4	− 433.984	+ 116.89	+ 99.43	+ 98.14	+ 96.54
5	− 389.523	+ 161.35	+ 130.32	+ 142.07	+ 127.34

higher energy isomers found. We verified that the Hartree–Fock calculations gave positive eigenvalues for the Hessian for all configurations, indicating that the isomers are also stable from the viewpoint of this calculation.

A comparison of the total energy differences between the lowest energy "natural" configuration and each isomer, for those isomers listed in Figs. 1–4 is given in Table 7. Notice that the energy ordering of the isomers is the same for all four calculations and that the three quantum calculations are in reasonable quantitative agreement for the energy differences of all isomers.

6. Summary and conclusions

We have made global searches for the stable isomers of adenine using a genetic algorithm combined with a force field potential. A large number of stable isomers were found, both planar and non-planar. Those configurations, which were similar to the natural configuration and stable were deemed interesting and were further studied with the PM3, Hartree–Fock and density functional approaches. The fact that minima of the potential model calculation were also geometrically close relatives of minima of the quantum calculations gives us confidence in the validity of using the potential approach as a first approximation for globally searching for isomers of adenine.

Since the isomers presented here have been found in four independent theoretical calculations and have been verified to be stable at both the classical and quantum level, we conclude that they may be observable in nature. Such results could have important implications in the biological activity of adenine and in the nano-electronic characteristics of adenine tied to metal nanoclusters and thus appear interesting enough for further detailed study.

Directions for future research include, calculating the free energies of the isomers at ambient temperatures, determination of the potential barriers between the isomers, including the base pair thymine and the DNA skeleton, applying the same global search to the other bases and base pairs, studying the binding of the isomers to metal nanoclusters and investigating the biological implications of the isomers.

Acknowledgements

The authors would like to thank R. Santamaria for useful comments on the draft. Financial support of DGAPA-UNAM grant IN101297, and CONACYT grant 25083E, and computing support of DGSCA-UNAM is gratefully acknowledged.

References

[1] J.P. Lewis, P. Ordejón, O.F. Sankey, Phys. Rev. B 55 (1997) 6880.
[2] R.P. Andres, T. Bein, M. Dorogi, S. Feng, J.I. Henderson, C.P. Kubiak, W. Mahoney, R.G. Osifchin, R. Reifenberger, Science 272 (1996) 1323.
[3] C.A. Mirkin, R.L. Letsinger, R.C. Mucic, J.J. Storhoff, Nature 382 (1996) 607.
[4] A.P. Alivisatos, K.P. Johnsson, X. Peng, T.E. Wilson, C.J. Loweth, M.P. Bruchez, P.G. Schultz, Nature 382 (1996) 609.
[5] I.L. Garzón, K. Michaelian, M.R. Beltran, A. Posada-Amarillas, P. Ordejón, E. Artacho, D. Sánchez-Portal, J.M. Soler, Phys. Rev. Lett. 81 (1998) 1600.
[6] V. Hrouda, J. Florián, P. Hobza, J. Phys. Chem. 97 (1993) 1542.

[7] R. Santamaria, A. Vazquez, J. Comp. Chem. 15 (1994) 981.
[8] S.J. Weiner, P.A. Kollman, D.T. Nguyen, D.A. Case, J. Comp. Chem. 7 (1986) 230.
[9] S.J. Weiner, P.A. Kollman, D.A. Case, U.C. Singh, C. Ghio, G. Alagona, S. Profeta Jr, P. Weiner, J. Am. Chem. Soc. 106 (1984) 765.
[10] F.E. Harris, in: F. Herman, A.D. McLean, R.K. Nesbet (Eds.), Computational Methods for Large Molecules and Localized States in Solids, Plenum Press, New York, 1973, p. 81.
[11] J. Holland, Adaptation in Natural and Artificial Systems, University of Michigan Press, Ann Arbor, 1975.
[12] B. Hartke, J. Phys. Chem. 97 (1993) 9973.
[13] J.T. Alander, An Indexed Bibliography of Genetic Algorithms in Chemistry and Physics (University of Vaasa, Finland, 1996) available via anonymous ftp: site ftp.uwasa.fi, directory cs/report94-1, file gaCHEMPHYSbib.ps.Z
[14] D.B. McGarrah, R.S. Judson, J. Comp. Chem. 14 (1993) 1385.
[15] R.S. Judson, M.E. Colvin, J.C. Meza, A. Huffer, D. Gutierrez, Int. J. Quan. Chem. 44 (1992) 277.
[16] K. Michaelian, Chem. Phys. Lett. 293 (1998) 202.
[17] P. Sutton, S. Boyden, Am. J. Phys. 62 (1994) 549.
[18] R.S. Judson, E.P. Jaeger, A.M. Treasurywala, M.L. Peterson, J. Comp. Chem. 14 (1993) 1407.
[19] K. Michaelian, Am. J. Phys. 66 (1998) 231.
[20] G. Chang, M. Lewis, Acta. Cryst. D50 (1994) 667.
[21] W.H. Press, S.A. Teukolsky, W.T. Vetterling, B.P. Flannery, Numerical Recipes in Fortran, 2, Cambridge University Press, Cambridge, 1992.
[22] M.J.S. Dewar, W. Thiel, J. Am. Chem. Soc. 99 (1997) 4907.
[23] J.J.P. Stewart, Comput. Chem. 10 (1989) 209.
[24] J.J.P. Stewart, MOPAC, v.6. Release for PC by L.A. Montero in the Laboratory of Computational and Theoretical Chemistry, Universidad de La Habana, 1993–1997.
[25] P. Culot, G. Dive, V.N. NGuyen, J.M. Ghuysen, Theor. Chim. Acta 82 (1992) 189.
[26] J. Baker, J. Comput. Chem. 7 (1986) 385.
[27] GAUSSIAN 94, Revision B.1, M.J. Frisch, G.W. Trucks, H.B. Schlegel, P.M.W. Gill, B.G. Johnson, M.A. Robb, J.R. Cheeseman, T. Keith, G.A. Petersson, J.A. Montgomery, K. Raghavachari, M.A. Al-Laham, V.G. Zakrzewski, J.V. Ortiz, J.B. Foresman, J. Cioslowski, B.B. Stefanov, A. Nanayakkara, M. Challacombe, C.Y. Peng, P.Y. Ayala, W. Chen, M.W. Wong, J.L. Andres, E.S. Replogle, R. Gomperts, R.L. Martin, D.J. Fox, J.S. Binkley, D.J. Defrees, J. Baker, J.P. Stewart, M. Head-Gordon, C. Gonzalez, J.A. Pople, Gaussian, Inc., Pittsburgh, PA, 1995.
[28] M.J. Frisch, A. Frisch, J.B. Foresman, Gaussian 94 User's Reference, Gaussian Inc., Pittsburgh, 1996, p. 111, and references therein.
[29] W. Kohn, L.J. Sham, Phys. Rev. 145 (1965) 561.
[30] P. Ordejón, E. Artacho, J.M. Soler, Phys. Rev. B 53 (1996) 10 441.
[31] D. Sánchez-Portal, P. Ordejón, E. Artacho, J.M. Soler, Int. J. Quantum Chem. 65 (1997) 453.
[32] N. Troullier, J.L. Martins, Phys. Rev. B 43 (1991) 1993.
[33] L. Kleinman, D.M. Bylander, Phys. Rev. Lett. 48 (1982) 1425.
[34] O.F. Sankey, D.J. Niklewski, Phys. Rev. B 40 (1989) 3979.
[35] R. Taylor, O. Kennard, J. Mol. Struct. 78 (1982) 1.